ELSEVIER

Journal of Nuclear Materials 241–243 (1997) 469–475

journal of nuclear materials

Erosion at the vessel walls of JET

M. Mayer [a,*], R. Behrisch [a], P. Andrew [b], A.T. Peacock [b]

[a] *Max-Planck-Institut für Plasmaphysik, EURATOM-Association, Boltzmannstrasse 2, D-85748 Garching, Germany*
[b] *JET Joint Undertaking, Abingdon, Oxfordshire OX14 3EA, United Kingdom*

Abstract

Erosion at the JET vessel walls has been investigated by means of carbon long term samples (LTS), partly covered with 530 nm Al and 750 nm Ni as well as implanted with Mo markers in a depth of 380 nm. The samples were exposed to JET plasmas between April–June 1995 (about 940 discharges). Upon removal, the surface layers of the LTS were analyzed with MeV ion beam techniques. On the inner torus walls, net erosion is found with an average of about 1.2×10^{15} Al-atoms/cm^2 and 9.4×10^{14} Ni-atoms/cm^2 per JET discharge, respectively. The erosion of carbon was $> 3.9 \times 10^{15}$ C-atoms/cm^2 per JET discharge. The erosion is due to sputtering by energetic charge-exchange neutrals emitted from the plasma during the discharge and He glow discharge cleaning between the discharges.

Keywords: JET; Impurity source; Erosion and particle deposition diagnostic; Erosion and particle deposition

1. Introduction

For a magnetically confined plasma the major plasma–material interaction takes place at limiters and divertor plates, which are hit directly by the particle and energy flux through the scrape off layer (SOL) plasma [1,2]. With the introduction of divertors the influx of impurities released at the target plates into the central plasma is largely reduced [3], especially if a low temperature and high density plasma can be achieved in front of the divertor plates [4]. With the reduction of the influence of divertor and limiter plates on the central plasma the plasma–material interactions at all other plasma facing areas of the vessel walls becomes the dominant processes for the introduction of impurities [5].

The plasma facing vessel walls of thermonuclear fusion experiments are bombarded with high fluences of energetic neutral hydrogen atoms created in charge-exchange collisions [6–9]. This bombardment causes an erosion of the vessel walls [6–11] and the introduction of impurity atoms into the plasma. The erosion by charge-exchange hydrogen is the dominant erosion mechanism at wall areas which are not hit directly by ions from the plasma [1,5]. Additionally the vessel walls are eroded by He glow discharge cleaning between the discharges.

In the joint European torus (JET) major parts of the vessel walls consist of Inconel. These parts are protected from the confined plasma by protection limiters made of carbon. During the last years of JET operation in addition beryllium has been routinely evaporated onto the vessel walls.

In this work the erosion at the vessel walls of JET has been investigated with long term samples (LTS), which have been installed and removed during major openings of the JET vessel [12]. The erosion of C, Al and Ni was measured with ion beam techniques.

2. Experimental

The LTS were mounted in a poloidal ring in octant 3 (outer wall) and octant 4 (inner wall) and in the toroidal direction in the torus midplane at the inner and outer walls [12]. The LTS were installed between the protection limiters directly at the vessel walls with good thermal contact to the wall. The temperature of the LTS can be taken to be the regular temperature of the wall, which is about 500 K. The LTS had an undisturbed line-of-sight to the plasma, but they were not hit directly by the plasma due to the limiters [12].

* Corresponding author. Tel.: +49-89 3299 1269; fax: +49-89 3299 1149; e-mail: mam@ipp.mpg.de.

PII S0022-3115(96)00548-X

The vessel walls were regularly conditioned with Be by routinely evaporating Be with 3 evaporators in octants 1, 5 and 7, which are located slightly below the torus midplane. The vessel walls were regularly conditioned by He glow discharge cleaning for about 18 h each week.

During this discharge period the divertor was Be. Most discharges start as a limiter plasma at the inner wall for about 10 s, followed by a divertor plasma. A typical JET discharge lasts for about 25 s.

The LTS were installed in April 1995 and were removed in June 1995. During this time about 940 discharges with a total discharge time of about 22500 s were performed. The plasma density was between $2-9 \times 10^{19}$ m^{-3} and the plasma current typically 3 MA. About 10% of the discharges were puffed with N_2.

All LTS were made of fine grain carbon with an exposed area of 60 mm^2. Two different sets of LTS were used. The first set consisted of samples where half of the sample was coated with 800 nm Al. The second set of LTS was coated with 530 nm of aluminum on one third of the sample surface, a further third was coated with 750 nm nickel, and the remainder of the sample was uncoated carbon with an Mo-marker implanted to a depth of 380 nm, thus allowing the measurement of the total erosion of these three materials. The surface layer composition as well as the thickness of the evaporated layers before and after installation in the JET vessel was measured by ion beam analysis on areas of typically 1 mm^2. The following surface analysis techniques have been applied:

- RBS (Rutherford backscattering spectroscopy) with 2.6 MeV ^{4}He ions and 2.3 MeV protons at a scattering angle of 165° giving a quantitative analysis of the thicknesses and compositions of the Al and Ni layers as well as the depth of the implanted Mo markers. The analysis depth with protons is > 10 μm.
- PIXE (proton induced X-ray emission) with 1.5 MeV protons giving a quantitative analysis of all elements with $Z > 10$ within a surface layer of several μm.
- NRA (nuclear reaction analysis) with 0.79 MeV ^{3}He ions by means of the D(^{3}He, α)p nuclear reaction at a scattering angle of 102.5° giving a quantitative analysis and depth profile of D in a surface layer of about 1.2 μm.
- ERDA (elastic recoil detection analysis) with 2.6 MeV ^{4}He ions at a scattering angle of 30°, allowing the detection of H and D in a surface layer of about 0.6 μm.

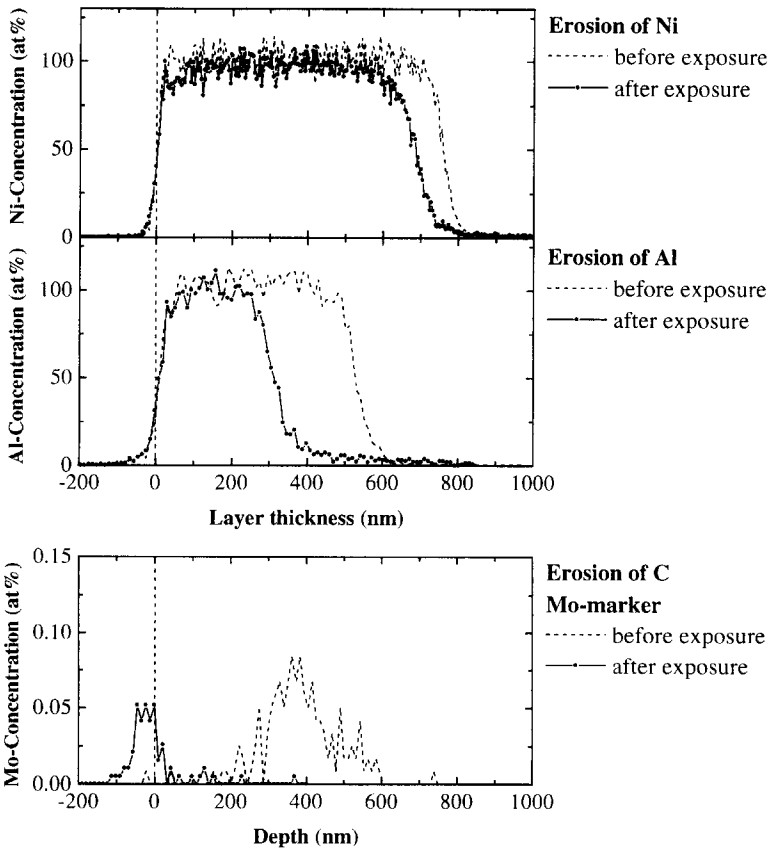

Fig. 1. Depth profiles of Ni, Al and the Mo marker implanted in C before (dashed) and after (full line and symbols) the exposition in JET. The depth profiles were measured by RBS with 2.6 MeV ^{4}He at 165°.

3. Results

3.1. Measured erosion of the LTS

Depth profiles of the Al and Ni layers, as well as a depth profile of the Mo markers before and after the exposure in JET from April–June 1995 are shown in Fig. 1 for a sample mounted at the inner wall. About 17% of the initial Ni-layer and about 60% of the initial Al-layer thickness were eroded. Some additional carbon in the range of several atomic percent is found in the Ni layer after exposition. Due to the additional carbon the decrease in the Ni layer thickness is less pronounced than in the case of the Al layers. In the case of carbon, the Mo-marker initially implanted to a depth of 380 nm, is found at the surface of the sample and is partly eroded. This means that all the carbon which was initially above the marker is eroded and only a lower limit for the erosion of carbon can be given.

All LTS installed at the inner wall showed erosion of the Al and Ni layers at an average rate of 1.2×10^{15} Al-atoms/cm^2 and 9.4×10^{14} Ni-atoms/cm^2 per discharge, respectively. The observed erosion rate of Al during the discharge period April–June 1995 is nearly the same as observed in earlier discharge periods from February 1994–March 1995. This is noteworthy because the Be-evaporator in octant 3 did not operate during the later discharge period resulting in a much smaller amount of evaporated Be on the LTS. Therefore the amount of evaporated Be at the inner wall seems to be low and does not influence the erosion measurements significantly.

The erosion of carbon was $> 3.9 \times 10^{15}$ C-atoms/cm^2 per discharge. LTS mounted in oct. 1, 5 and 8 at the inner wall in the torus midplane showed within 30% the same amount of erosion of C, Al and Ni as the samples mounted in octant 4 at the inner wall, see Figs. 2 and 3.

LTS mounted at the outer wall in octant 3 (no evaporator) showed minor deposits (maximum about 80 nm) and in some cases erosion, see Fig. 2. The deposited layers consist mainly of Be, C and O with varying composition. N, P, S, Cl, K, Ca, Ti, Cr, Fe and Ni were detected as traces, typically below 2×10^{16} atoms/cm^2. LTS mounted

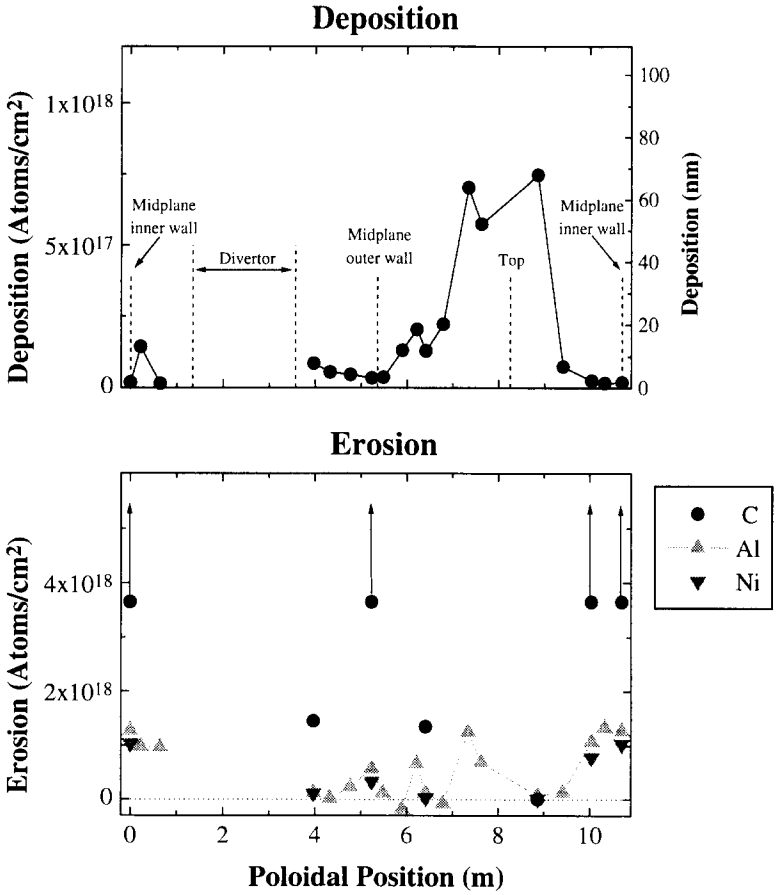

Fig. 2. Poloidal distribution of the total deposition of all elements (top) and erosion of C, Al and Ni (bottom). For C in some cases only a lower limit of the eroded amount can be given. These samples are marked with an arrow. Samples at the inner wall were mounted in octant 4, samples at the outer wall were mounted in octant 3.

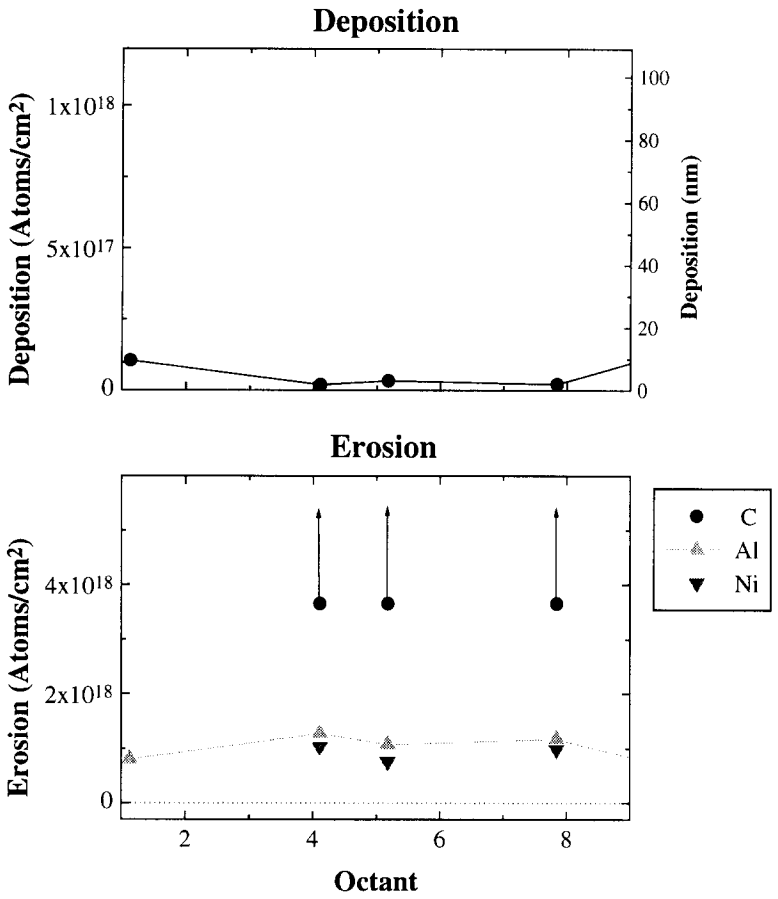

Fig. 3. Toroidal distribution of the total deposition of all elements (top) and erosion of C, Al and Ni (bottom) at the inner wall. For C in some cases only a lower limit of the eroded amount can be given. These samples are marked with an arrow.

in oct. 1, 5 and 8 at the outer wall in the torus midplane showed no erosion but deposited layers up to 3 μm consisting mainly of Be.

3.2. Estimation of an upper bound for the CX-flux

The erosion measured at the LTS is due to sputtering with energetic CX neutrals during the discharges and additionally to He glow discharge cleaning. The measured erosion of the LTS has been used to get an estimate of an upper bound for the integral neutral CX flux.

For an incident flux with energy and angular distribution $\Gamma(E, \phi)$ an effective sputtering yield Y_{eff} can be defined by

$$Y_{\text{eff}} = \frac{1}{\Gamma_{\text{tot}}} \int \mathrm{d}E \int \mathrm{d}\phi\, Y(E, \phi)\Gamma(E, \phi), \qquad (1)$$

where $Y(E, \phi)$ is the energy and angular dependent sputtering yield and Γ_{tot} the total incident flux, $\Gamma_{\text{tot}} = \int \mathrm{d}E \int \mathrm{d}\phi\, \Gamma(E, \phi)$. The main contribution to the sputtered flux is due to incident deuterium in the energy range 50–500 eV [7,11]. These particles originate mainly from the scrape-off layer [13]. Because at JET the CX-measurements are only performed in the keV-range and there are large uncertainties in theoretical calculations with neutral gas codes, we have taken an energy spectrum of the CX-flux measured at ASDEX Upgrade during a standard shot (#6535, $n_e = 3 \times 10^{19}$ m^{-3}). The spectrum is shown in Fig. 4. At ASDEX Upgrade the energy distribution of the CX-flux is measured in detail with the low energy neutral particle analyzer (LENA) in the energy range 30–1000 eV [14,13,15] and with the neutral particle analyzer (NPA) for energies > 500 eV [16,13]. The flux below 30 eV is based on a simulation with the EIRENE code [17–19].

It should be noted that for different discharge conditions (Ohmic discharge, H-mode with and without gas puff) the total flux may vary strongly, however the effective sputtering yield Y_{eff} calculated from Eq. (1) changes only about 30% for low and medium-Z elements for the different discharge conditions. This is also the case for preliminary calculations of the CX spectra for ITER [20].

Table 1
Effective sputtering yields Y_{eff} for the bombardment of Be, C, Al and Ni by D. Energy distribution of the incident flux as in Fig. 4. For C only physical erosion and physical plus chemical erosion at 500 K is given. For Al experimental values of the sputtering yield including a layer of Al_2O_3 on the surface were used

Material	Y_{eff}
Be	1.3×10^{-2}
C (phys.)	7.5×10^{-3}
C (500 K)	2.0×10^{-2}
Al	5.9×10^{-3}
Ni	7.8×10^{-3}

The calculated values of Y_{eff} using the sputtering data for normal incidence from Ref. [21] are shown in Table 1. The sputtering yields in this energy range are known with an error of about 20–30%. In the case of Al oxygen was always present on top of the Al coating of the LTS. Experimentally determined sputtering yields include also an Al_2O_3 layer on top of Al and were used for the calculation of Y_{eff}.

One uncertainty in the calculation of Y_{eff} is the angular distribution of the incident flux. The maximum in the angular distribution of the CX-flux might be at an angle of about 40–50° [22]. The sputtering yields for Al and Ni at 40° are about 1.5–2 times higher than the sputtering yields at normal incidence [21].

Under the given assumptions the total CX-flux to the inner wall of the JET torus can be obtained from the erosion of the Al and Ni layers measured on the LTS. The resulting mean CX-flux to the inner wall is 1.6×10^{17} D-atoms cm^{-2} per discharge. Because of the different phases of the discharge (first limiter plasma, then divertor plasma) only a mean CX-flux for the whole discharge can be given. Due to the uncertainty of the angular distribution (higher sputtering yields for oblique incidence) and the additional erosion by He glow discharge cleaning the obtained value for the total CX-flux overestimates the total neutral CX flux and can be only taken as an upper bound.

The measured erosion of carbon and the erosion calculated for a mean CX-flux of 1.6×10^{17} D-atoms cm^{-2} per discharge are compared in Table 2. The measured total erosion of carbon was $>3.6\times10^{18}$ C-atoms/cm^2. Because the whole carbon layer above the Mo marker was eroded, this is only a lower limit for the total erosion. The effective sputtering yields Y_{eff} for physical erosion and physical plus chemical erosion are given in Table 1. If we assume only physical sputtering of carbon [21] the erosion

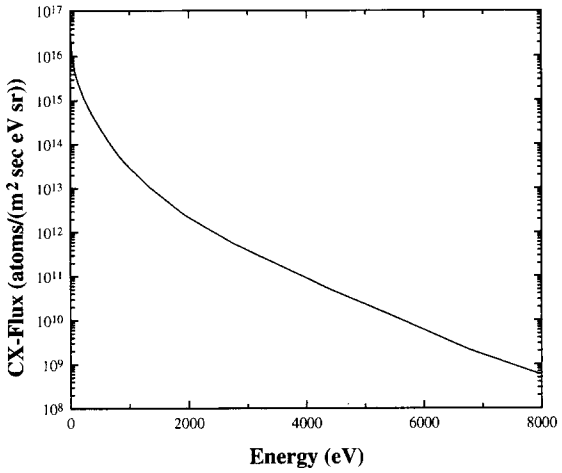

Fig. 4. Deuterium charge-exchange flux to the outer wall of ASDEX Upgrade. Standardshot #6535, $n_e\times10^{19}$ m^{-3}.

should be 1.1×10^{18} C-atoms/cm^2. This is a factor of about 3 lower than the measured erosion. Physical sputtering of carbon alone is therefore not sufficient to explain the measured erosion.

Physical and chemical erosion of carbon was calculated using the formalism developed in Ref. [23]. It should be noted that the flux density of the CX-flux is not much higher than obtained in laboratory experiments. The uncertainty of the sputtering yields due to the flux density dependence therefore is low.

The calculated erosion including chemical and physical sputtering is 3×10^{18} C-atoms/cm^2, which agrees within the uncertainties with the measured erosion of carbon. This suggests that the main contribution to the erosion of carbon at the JET vessel walls is therefore chemical erosion.

3.3. Total erosion at the vessel wall

Assuming toroidal symmetry, we can use the measured erosion of the LTS to calculate the total amount of eroded material from the vessel walls.

The exposed metal area of the inner wall has an area of about 15 m^2. At the whole inner wall net erosion is observed. The measured erosion of Ni with the LTS is about 8.8×10^{17} atoms/cm^2 during this discharge period. The sputtering yields of the Inconel vessel walls and of Ni are nearly equal. During the discharge period from April–June 1995 therefore in total about 1.3×10^{23} atoms (13 g Inconel) were eroded from the inner wall.

Table 2
Measured and calculated erosion of carbon on the LTS for a total CX-flux of 1.5×10^{16} D-atoms cm^{-2} s^{-1}

Measured erosion (C-atoms/cm^2)	Physical sputtering (C-atoms/cm^2)	Physical + chemical sputtering (C-atoms/cm^2)
$>3.6\times10^{18}$	1.1×10^{18}	3.0×10^{18}

The major part of the outer wall is covered with Be due to the Be evaporations, except at areas shadowed from the evaporation. Due to the inhomogeneous Be coverage the erosion of Ni, Fe and Cr from the Inconel vessel wall at the outer side of the torus cannot be determined. However, it appears that the major source of Ni, Fe and Cr is the inner wall because of the more effective Be evaporation at the outer wall.

A small amount of the eroded Ni, Fe and Cr is redeposited at the vessel walls and can be found on LTS in deposition dominated areas at the outer wall. The amount of deposited Ni, Fe and Cr is typically about 1.4×10^{16} atoms/cm^2. The deposition dominated wall area is about 130 m^2. The total amount of redeposited Ni, Fe and Cr is therefore about 2×10^{22} atoms, which is about 15% of the amount of eroded Inconel. More than 80% of the eroded Inconel is most likely ionized in the scrape-off layer and deposited at the carbon limiters or transported into the divertor, where thick deposits are observed [24].

An upper limit for the total erosion of Be can be estimated in the following way: The total wall area of JET is about 200 m^2. The effective sputtering yield Y_{eff} for sputtering of Be with D is 1.3×10^{-2} (Table 1). Assuming a spatially homogeneous flux of 1.6×10^{17} D-atoms cm^{-2} per discharge to the walls totally covered with Be the sputtered flux of Be is of the order 4×10^{21} Be-atoms per discharge. This value is an upper limit, because

1. The CX-flux at the inner midplane cannot be extrapolated to the whole of the vessel. In particular during the initial start-up phase of the plasma the plasma rests at the inner wall.
2. Not all wall areas (for example the inner wall, but also areas that are shadowed from the Be evaporation) are covered with Be.

4. Conclusions

The erosion of long term samples (LTS) mounted at the vessel walls of JET between protection limiters is due to the bombardment by energetic neutral deuterium atoms created in charge-exchange collisions during the discharges and additionally to He glow discharge cleaning between the discharges. On the inner torus walls, net erosion is found to a level of about 1.2×10^{15} Al-atoms/cm^2 and 9.4×10^{14} Ni-atoms/cm^2 per JET discharge, respectively. An upper bound for the charge-exchange neutral flux to the inner torus wall can be estimated from the measured erosion of the Al and Ni layers to be about 1.6×10^{17} D-atoms cm^{-2} per discharge. The measured erosion of carbon ($> 3.9 \times 10^{15}$ C-atoms/cm^2 per JET discharge at the inner wall) is mainly due to chemical erosion of carbon. Physical sputtering of carbon alone can explain only about 35% of the observed carbon erosion.

During one JET discharge about 2.9×10^{20} Ni, Fe and Cr-atoms are sputtered from the inner Inconel vessel wall. About 15% of the sputtered wall material is redeposited at the outer torus walls, while the rest is likely redeposited either locally at the limiters or at the divertor plates. The total amount of beryllium sputtered from the vessel walls is $\leq 4 \times 10^{21}$ atoms during one JET discharge. All impurity fluxes are upper bounds because of the additional effect of He glow discharge cleaning.

In ITER the CX-sputtering at the walls will be an impurity source as well. In order to reduce the erosion at the walls and the influx of impurities from the walls into the plasma the CX-flux has to be reduced. The CX-fluxes to the vessel walls of ITER are predicted to be lower by a factor of about 10 than the CX-flux measured at the inner wall of JET, but may be as high as observed at JET. The measured erosion at the vessel walls of JET may be therefore taken as an upper limit for the expected erosion at the vessel walls of ITER.

Acknowledgements

The Mo-implantation was kindly performed by J. Schöneich at Institut für Ionenstrahlphysik und Materialforschung, Forschungszentrum Rossendorf/Dresden. The providing of CX-spectra measured at ASDEX Upgrade by J. Stober and H.-U. Fahrbach and the help of C. Fritsch in performing the RBS measurements is gratefully acknowledged.

References

[1] G. McCracken, Plasma Phys. Controlled Fusion 29 (1987) 1273.
[2] G. Matthews, S. Fielding, G. McCracken, D. Goodall, C. Pitcher, P. Stangeby, J. Allen, R. Barnsley, R. Bissel, N. Hawkes, J. Hugill, P. Johnson, L. Khimchenko and A. Ternopol, Nucl. Fusion 28 (1988) 2209.
[3] M. Keilhacker and K. Lackner, J. Nucl. Mater. 111–112 (1982) 370.
[4] A. Kallenbach, R. Dux, V. Mertens, O. Gruber, G. Haas, M. Raufmann, W. Poschenrieder, F. Ryter, H. Zohm, M. Alexander, K. Behringer, M. Bessenrodt-Weberpals, H. Bosch, K. Büchl, A. Field, J. Fuchs, O. Gehre, A. Herrmann, S. Hirsch, W. Köppendörfer, K. Lackner, K. Mast, G. Neu, J. Neuhauser, S. de Pena Hempel, G. Raupp, K. Schönmann, A. Stäbler, K. Steuer, O. Vollmer, M. Weinlich, W. West, T. Zehetbauer and the ASDEX Upgrade Team, Nucl. Fusion 35 (1995) 1231.
[5] J. Roth and G. Janeschitz, Nucl. Fusion 29 (1989) 915.
[6] H. Verbeek and the ASDEX-team, J. Nucl. Mater. 145–147 (1987) 523.
[7] R. Behrisch, J. Roth, G. Staudenmaier and H. Verbeek, Nucl. Instr. Methods B 18 (1987) 629.
[8] H. Verbeek, V. Dose, J. Fu, O. Gehre, J. Gernhardt, G. Janeschitz, E. Müller, H. Röhr, K. Steuer, F. Söldner and the ASDEX-team, J. Nucl. Mater. 162–164 (1989) 557.
[9] G. Staudenmaier and W. Wampler, J. Nucl. Mater. 162–164 (1989) 414.

[10] J. Roth, J. Ehrenberg, K. Wittmaack, P. Coad and J. Roberto, J. Nucl. Mater. 145–147 (1987) 383.
[11] C. García-Rosales, J. Nucl. Mater. 211 (1994) 202.
[12] M. Mayer, R. Behrisch, V. Prozesky, P. Andrew and A. Peacock, in: 22nd EPS Conf. on Controlled Fusion and Plasma Physicseurophysics conference abstracts, Vol. 19C (1995) p. 301.
[13] H. Verbeek, O. Heinrich, R. Schneider, H. Fahrbach, W. Herrmann, J. Neuhauser, U. Stroth, the ASDEX-team and D. Reiter, J. Nucl. Mater. 196–198 (1992) 1027.
[14] H. Verbeek, J. Phys. E 19 (1986) 964.
[15] H. Verbeek and A. Schiavi, The Low Energy Neutral Particle Analyser (LENA) at W7-AS, Technical Report IPP 9/103, Max-Planck-Institut für Plasmaphysik, Garching (1994).
[16] H. Fahrbach, W. Herrmann and H. Mayer, in: 16nd EPS Conf. on Controlled Fusion and Plasma Physicseurophysics conference abstracts, Vol. 13B (1989) p. 1537.
[17] D. Reiter, Technical Report Jül-1947, Forschungszentrum Jülich (1984).
[18] D. Reiter, The EIRENE Code, Users Manual, Technical Report Jül-2599, Forschungszentrum Jülich (1992).
[19] J. Stober, H. Verbeek, D. Coster, H.-U. Fahrbach, O. Heinrich, W. Herrmann, G. Haas, O. Kardaun, D. Reiter, R. Schneider, J. Schweinzer, W. Suttrop, ASDEX Upgrade Team, NI Team, ICRH Team and ECRH Team, in: 22nd EPS Conf. on Controlled Fusion and Plasma Physicseurophysics conference abstracts, Vol. 19C (1995) p. 249.
[20] A. Kukushkin (1995), private communication.
[21] W. Eckstein, C. García-Rosales, J. Roth and W. Ottenberger, Sputtering Data, Technical Report IPP 9/82, Max-Planck-Institut für Plasmaphysik, Garching (1993).
[22] J. Roth, in: Physics of Plasma–Wall Interactions in Controlled Fusion, eds. D. Post and R. Behrisch, NATO ASI Series B, Vol. 131 (Plenum Press, New York, London, 1986).
[23] J. Roth and C. García-Rosales, Analytic Description of the Chemical Erosion of Graphite by Hydrogen Ions, J. Nucl. Mater. (1996), accepted for publication.
[24] J. Coad, J. Nucl. Mater. 226 (1995) 156.